RESEARCH PAPER

An Inverse Method to Estimate Cowper-Symonds Material Model Parameters from a Single Split Hopkinson Pressure Bar Test

C. Hernandez[1] · D. L. Blanco[1] · A. Maranon[2]

Abstract
This paper presents the estimation of the parameters of the Cowper-Symonds material model of a commercial copper alloy from a single Split Hopkinson Pressure Bar Test using an inverse method. Parameters were identified by minimizing the error between the transmitted strain signal predicted by a finite element model and those observed experimentally. The Taylor Test was used to validate the identified parameters by comparing the experimental final length of impacted specimens and the ones predicted by a finite element model using the identified parameters. Also, identified parameters were contrasted with those found by a traditional curve-fitting approach. It was found that finite element models using the identified parameters are better able to predict plastic deformation than those using parameters from traditional curve-fitting.

Keywords UNS C83600 · Mechanical characterization · High-strain rates · Split Hopkinson Pressure Bar Test · Taylor test · Inverse problem · Parameter identification

Introduction

Identifying material parameters at a high strain-rate is essential in determining material behavior and mechanisms involving dynamic loading and plastic deformation. Therefore, the mechanical response of many materials has been investigated using diverse techniques to determine the mechanical properties under high strain loading [1–4]. This mechanical characterization is built on estimating material parameters associated with a phenomenological constitutive model from data obtained from dynamic experiments using mixed numerical-experimental methods-also called inverse methods for material parameter identification. In these methods, parameter estimation is carried out by minimizing the error between the responses predicted by a numerical model and those observed experimentally [5]. For example, Mariani and Gobat [6] adopted an inverse approach based on a Sigma-point Kalman filter to identify quasi-brittle materials' material properties using spall tests. Similarly, Vaz and Tomiyama [7] presented an inverse procedure to identify stainless steel material parameters. Identifying inelastic parameters was based on multiple mechanical tests using optimization techniques.

There are a number of experimental techniques available to test materials at high strain rates, from drop-weight machines (10–10^3 s^{-1}) to shock loading by plate impact test (10^6–10^8 s^{-1}) [8]. Although one of the most widely used experimental techniques employed to test materials at a high strain rate is the Split Hopkinson Pressure Bar (SHPB) (10^3–10^4 s^{-1}), [9]. This test can reconstruct the stress–strain curve at high strain rates of diverse materials, becoming one of the most used methods for obtaining materials' mechanical behavior at high strain rates.

However, the material parameters' determination from the experimental data yielded by SHPB tests or similar impulsive tests [10] is an open research problem in the literature. There is no standardized method to determine material parameters from the experimental data; on the contrary,

✉ C. Hernandez
    camilo.hernandez@escuelaing.edu.co

    D. L. Blanco
    david.blanco@escuelaing.edu.co

    A. Maranon
    emaranon@uniandes.edu.co

[1] Sustainable Design in Mechanical Engineering Research Group (DSIM), Mechanical Engineering, Escuela Colombiana de Ingeniería Julio Garavito, AK 45 205-59, 111166 Bogota, Colombia

[2] Structural Integrity Research Group, Mechanical Engineering Department, Universidad de los Andes, CR 1 ESTE 19A 40, 111711 Bogota, Colombia

several proposed methodologies in the literature have been devised to post-process experimental data to estimate material parameters. These characterization methodologies break away from traditional curve-fitting methods to implement optimization problems. For example, Sasso et al. [11] proposed an optimization procedure to determine, from tension SHPB tests, the material parameters based on a finite element model. Likewise, Sedighi et al. [12] proposed a characterization method to determine material parameters using an optimization approach of SHBP tests against finite element models. Another approach was presented by Milani et al. [13]. Using a weighted multi-objective identification strategy, they presented a method to determine the material parameters from SHPB tests. This strategy allows for determining the Johnson-Cook material parameters and simultaneously detecting their interaction.

This paper presents an inverse method for estimating the parameters of the Cowper-Symonds material model of a red bronze from a single Split Hopkinson Pressure Bar Test. The identified parameters were compared with those found by a traditional curve-fitting approach. Finally, the effectiveness of the proposed method was measured by the fitness of the characterized constitutive model to predict the essential deformation physics at high-strain rates during Taylor Tests at different strain rates.

Materials and Methods

Material

The material characterized in this work was a commercially available round rod bronze, which is usually employed to manufacture couplings, fasteners, bushings, marine products, and pipe fittings. Chemical composition analysis was performed according to ASTM E478 standard [14]. The material was found to be a copper alloy UNS C83600 compared to ASTM B62 designation [15] as shown in Table 1. A density of 8913 kg/m^3 was obtained by the water displacement method.

Quasi-static Compression Tests

Compression tests according to ASTM E9-09 standard [16] were performed to determine the mechanical properties at quasi-static range. Compression tests were performed on a universal testing machine under standard laboratory conditions (23 $\pm$ 1°C and 50 $\pm$ 5% relative humidity). Solid cylindrical short test specimens with dimensions according to the standard were used: Diameter 13.0 mm, Length 25.0 mm. A crosshead speed of 4 mm/min was used during the test. Three specimens were tested to determine the elastic modulus E, yield stress σ_0, tangent modulus E_{tan}, maximum stress σ_{max} and fracture strain ε_f.
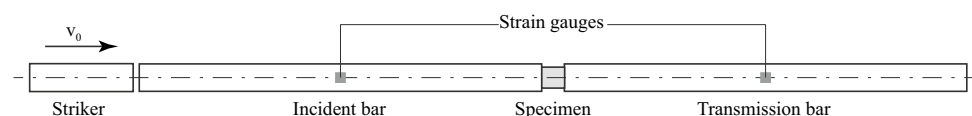
Split Hopkinson Pressure Bar Test

Split Hopkinson Pressure Bar (SHPB), also known as Kolsky bar, is an experimental tool proposed by Kolsky [17] based on an extension of the Hopkinson technique [18]. This device is widely used to obtain the dynamic response of materials at high strain rates, ranging from 10^2 to 10^4 s^{-1}, by subjecting the material specimen to pulse stresses [19].

The typical SHPB apparatus consists of three essential components as shown in Fig. 1: a striker or loading bar, an incident bar or input bar, and a transmitter bar or output bar. All bars are fabricated from the same material and diameter. The test specimen is placed between both bars. The striker is launched at a constant speed, usually using a gas gun, to impact the incident bar. A compressive stress wave is generated on the incident bar and propagated through the length of the rod. When the stress pulse reaches the specimen, part of it is reflected in the incident bar, and the rest transmits into the specimen. The pulse wave reverberates inside the specimen, compressing it. Then, the remaining part of the pulse wave is transmitted to the output bar. Strain gauges on the bars' surface conditioned with a Whetstone bridge are used to capture the stress waves transmitted through both bars as strain signals. The captured strain signals are processed to obtain the strain-stress relation of the tested material.

In this work, four SHPB tests were performed without pulse shaper on the copper alloy at different impact

Table 1 Chemical composition of copper alloy sample and UNS C83600 chemical requirements [15]

wt%	Sample	C83600
Cu	84.04	84.0–86.0
Sn	3.16	4.0–6.0
Pb	7.51	4.0–6.0
Zn	3.90	4.0–6.0
Ni	0.09	1.0
Fe	0.19	0.3
Sb	0.19	0.25
S	0.03	0.08
P	0.001	0.05
Al	0.00	0.005
Si	0.01	0.005

Fig. 1 Illustration of SHPB apparatus

Table 2 SHPB apparatus dimensions

Incident bar length	2.54 m
Transmission bar length	2.0 m
Bars diameter	20.5 mm
Striker length	231 mm
Striker Diameter	20.5 mm

Table 3 Specimen dimensions and impact speed for SHPB tests

Test	Average strain rate (s^{-1})	Maximum strain rate (s^{-1})	Specimen length (mm)	Specimen diameter (mm)	Impact velocity (m/s)
1	1322	2168	8.0	16.0	17.34
2	2714	4165	8.0	16.0	33.32
3	4325	5516	5.0	10.0	27.58
4	4921	6708	5.0	10.0	33.45

velocities. The dimensions of the SHPB device used are shown in Table 2. The bars were manufactured of martensitic chromium stainless steel Böhler M303 that offers high toughness. General purpose uniaxial strain gages with 0.125-inch length and 350 Ω connected to a 2310B signal conditioning amplifier system by Vishay Precision Group were used to capture the waves on the surface of incident and transmission bars. Manual alignment of the bars was performed until the amplitude of reflected signal during an empty test (test without specimen) is below 5% of the amplitude of incident wave. Low viscosity mineral oil was used to lubricate all contact interfaces between bars and specimen to promote wave transmission and reduce friction. Incident, transmitted and reflected pulses were acquired in each test at a sampling rate of 200 MS/s. Classical two-wave method was used for data processing and obtain stress-stain curves. No dispersion correction was used. Dimensions of the specimen and impact velocity of the striker for each test are shown in Table 3. Average strain rates of 1322 s^{-1}, 2714 s^{-1}, 4325 s^{-1} and 4921 s^{-1} were achieved.

Taylor Test

Taylor impact test, also known as the Taylor cylinder test or Taylor anvil test, is an experimental technique devised to estimate the average dynamic yield strength of materials at high strain rates in the range of 10^3 s^{-1} to 10^4 s^{-1}. This technique was proposed in the 1940s by Taylor [20], and since, it has become a common procedure to verify the constitutive behavior of materials [21].

The Taylor test consists of impacting a short right circular cylinder, with a length-to-diameter (L_0/D_0) ratio of 3 to 5, against a massive rigid anvil. The altered geometry

of the specimen after the impact (i.e., the final length L_f, the undeformed length X, and the deformed diameter D_f) is related to the average dynamic yield strength of the material through analytical analysis of the dynamic deformation and wave propagation during the impact. This analysis was initially developed by Taylor [20] and then improved by Whiffin [22], Wilkins and Guinan [23], and Hawkyard [24]. Figure 2 shows a schematic of the Taylor impact test before and after deformation.

In this work, five Taylor tests were performed at different impact velocities, where cylindrical specimens were fired onto a 30 mm hardened steel plate using a gas gun. Specimens dimensions, impact velocities, and strain rates for each Taylor test are shown in Table 4. Average strain rate $\dot{\varepsilon}_{avg}$ for each impact was calculated using Eq. 1 [20]. After impact, the specimens' final length and diameter were measured to calculate the dynamic yield strength σ_y. Dynamic yield strength for each strain rate was calculated using Eq. 2 [23]. In both equations, v_0 is the impact velocity, L_0 is the initial specimen length, X is the undeformed length of the specimen, and ρ_0 is the density of the material.

$$\dot{\varepsilon}_{avg} = \frac{v_0}{2(L_0 - X)} \tag{1}$$

$$\ln\left(\frac{L_f}{L_0}\right) = -\frac{\rho_0 v_0^2}{2\sigma_y} \tag{2}$$

Constitutive Model: Plastic Kinematic Model

The selected constitutive material model used to describe the copper alloy's mechanical behavior is the Plastic Kinematic Model [25] with kinematic hardening only, which is based on the Cowper-Symonds constitutive material model [26]. This bilinear elastoplastic model describes the constitutive behavior of the material by two straight lines. First, the mechanical behavior is defined by a lineal elastic zone characterized by the Elastic Modulus E that reaches the dynamic yield stress σ_y. The dynamic yield stress is dependent on the strain rate and is scaled by two phenomenological material parameters as shown in Eq. 3, where σ_0 is the initial yield stress determined at quasi-static range, $\dot{\varepsilon}$ is the strain rate, and C and P are the phenomenological Cowper-Symonds strain rate parameters. From the dynamic yield stress, the plastic strain regime starts defined by the slope of the strain-hardening line and is given by the tangent modulus E_{tan}. Then, five material parameters should be determined to characterize the copper alloy's mechanical behavior: the elastic modulus E, the initial yield stress σ_0, the tangent modulus E_{tan} and two Cowper-Symonds parameters C and P. The Poisson's ratio for this alloy is assumed as 0.34.

Fig. 2 Schematic of the Taylor impact specimen before and after impact

Initial State

Final State
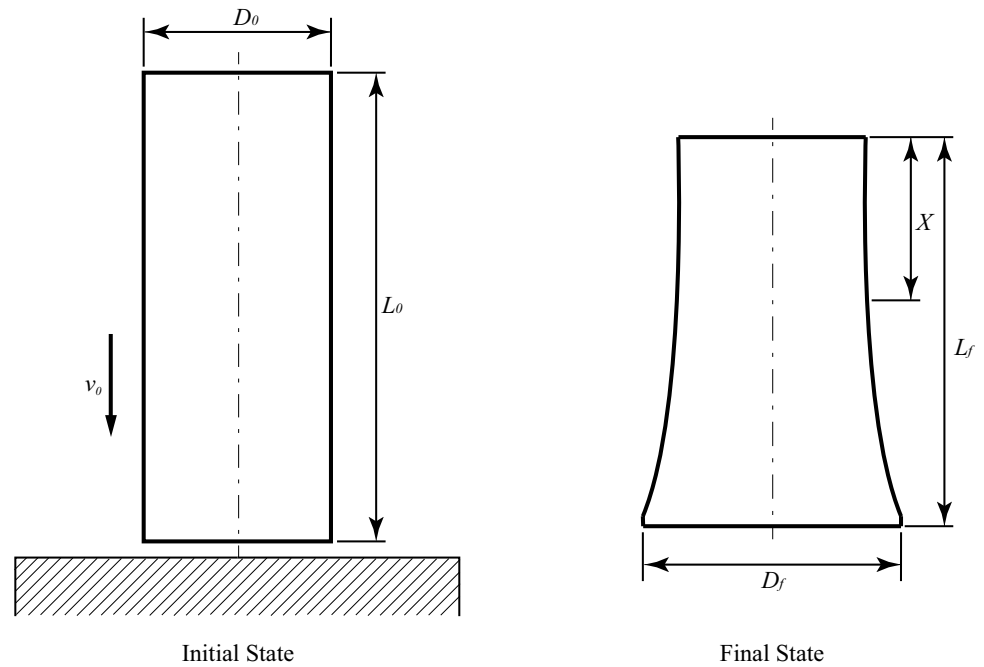
Table 4 Specimen dimensions and impact velocity for Taylor tests

Test	Specimen length (mm)	Specimen diameter (mm)	Impact velocity (m/s)
1	25.56	8.50	101.56
2	25.58	8.50	112.87
3	25.71	8.50	123.70
4	25.55	8.50	131.47
5	25.53	8.49	144.73

$$\sigma_y = \sigma_0 \left[1 + \left(\frac{\dot{\varepsilon}}{C} \right)^{\frac{1}{P}} \right] \tag{3}$$

Constitutive Model Characterization

An inverse computational procedure to characterize the copper alloy's constitutive behavior from a single SHPB test was developed in this research and written by the authors on the Ansys Parametric Design Language (APDL). Similar methods developed by the authors of this paper to characterize materials from Taylor tests and Drop tests have been published elsewhere [27, 28]. These methods were validated by determining their capability to predict the plastic-strain distribution inside the deformed material [29].

The procedure proposed in this paper was formulated as a first-class inverse problem of the SHPB test. This problem consists of determining the material parameters ($\vec{z}$) associated with a given constitutive model by minimizing the difference between the strain signal captured during an SHPB test (u_0) and the computed strain signal from a reference model of the SHPB test ($u(\vec{z})$). The reference model, in this case, corresponds to a finite element simulation of the SHPB using material trial parameters ($\vec{z}$). This optimization problem yields the set of material parameters when Eq. 4 is minimum. This equation represents the mean squared error between the computed and experimental strain signals.

$$\phi(\vec{z}) = \frac{1}{n} \sum_{i=1}^{n} \left([u(\vec{z})] - [u_0] \right)^2 \tag{4}$$

Figure 3 presents a six-step computational procedure to solve this inverse problem. The basic steps are: (1) A SHPB test is performed on the material. Transmitted pulse strain signals are captured and used as input for the material parameters optimization process. (2) A computational data reduction operator is applied to help the signal comparison based on central line moments. (3) A finite element model of the SHPB test is implemented using material trial parameters to compute the transmitted pulse. (4) Central line moments of the computed transmitted pulse are calculated. (5) An objective function is assembled as the difference between the central line moments computed from the finite element model and central line moments from experimental measurements. (6) A genetic algorithm minimizes the objective function and determines the optimum set of material parameters. The inverse computational characterization procedure yields as result the optimum set of material parameters $\vec{z} = [k_1, k_2, \dots, k_n]$. This set of material parameters minimizes the differences between the finite element

Fig. 3 Inverse computational procedure for determining material parameters from a SHPB test
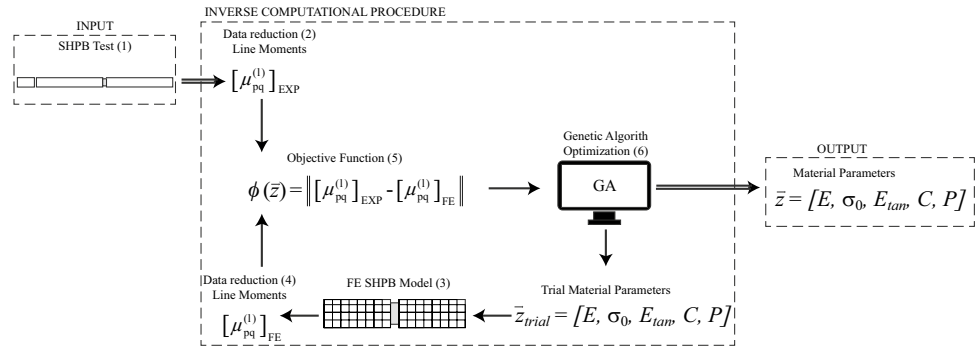
model and the experimental measurements of an SHPB test. Further details of the inverse computational characterization procedure, including the data reduction operator based on line moments and the optimization by a genetic algorithm, can be found in [27–29].

One of the critical steps during the computational procedure is the data reduction process made to the SHPB signal to efficiently compare the results of the experimental test and the computational simulations. The data reduction technique used in this work is based on the computation of the Line Moments of the SHPB. For the processing of these kinds of data Lambert and Gao [30] design the Line Moments for identification problems where contours represented by lines are used. The concept of Line Moments is an extension of the Geometrical Moments proposed by Hu [31] to represent the contour data of a scene by a reduced set of parameters. The Geometric Moments are invariants used in image analysis to represent patterns contained in images. This approach consists in representing images by a set of its two-dimensional moments with respect to a fixed coordinate system. Since then, Geometrical Moments have been used in pattern recognition, face recognition, ship and aircraft identification and many image analysis applications. In the specific case of Line Moments, the applications have focused on the identification of boundaries, shape description and signal recognition, like the inspections of parts [32].

Line moments were defined mathematically by Lambert and Gao [30] in terms of a contour integral as shown in Eq. 5. Where $p, q = 0, 1, 2, \ldots n$; s is the arc length and $f(s)$ is the linear density, which can be set to $f(s) = 1$ in the case of describing the contour shape. A uniqueness and existence theorem demonstrated by Hu [31] for geometric moments, is also extended to line moments. It states that assuming a contour C piecewise, continuous, bounded and with non-zero values only in finite part of the xy plane, moments m_{pq} of all orders exist and are uniquely determined by C and conversely.

$$m_{pq}^{(l)} = \int_C x(s)^p y(s)^p f(s)ds. \tag{5}$$

On the other hand, Line Moments $m_{pq}^{(l)}$ are dependent on the selection of the coordinate system used for their calculation. Therefore, to obtain invariance under translation, the Central Line Moments $\mu_{mp}^{(l)}$ are proposed to calculate the Line Moments with is coordinate system shifted to the contour centroid $(\bar{x}, \bar{y})$.

The Central Line Moments are defined as follows:

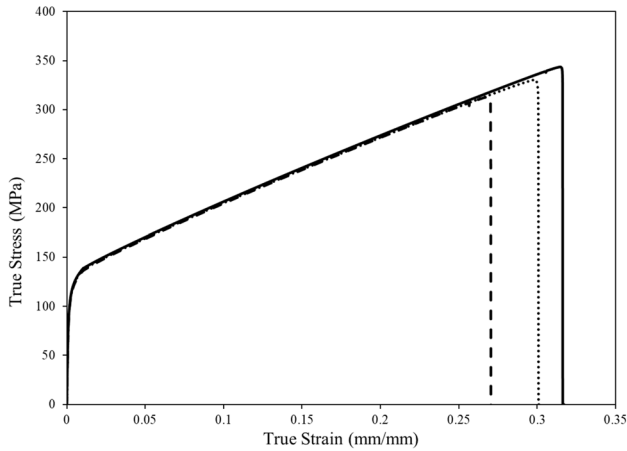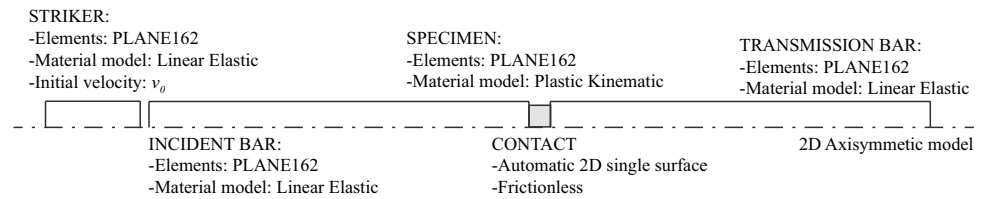$$\mu_{pq}^{(l)} = \int_C (x(s) - \bar{x})^p (y(s) - \bar{y})^p f(s)ds, \tag{6}$$

with

$$\bar{x} = \frac{m_{10}^{(l)}}{m_{00}^{(l)}}; \bar{y} = \frac{m_{01}^{(l)}}{m_{00}^{(l)}}. \tag{7}$$

Finite Element Model of the SHPB Test

The inverse computational characterization procedure determines the material parameters by minimizing the difference between the measured transmitted pulse and a numerical simulation of the SHPB test. Therefore, using an explicit solution scheme, a numerical model representing the SHPB test was implemented in the software ANSYS/LS-DYNA. Due to the event's symmetry, the test was modeled using 2D axisymmetry with 2D structural solid elements (PLANE162) with a quadrilateral shape, four nodes, and six degrees of freedom per node. The bars and striker of the SHPB test were modeled as isotropic linear elastic solids with steel properties. Elastic modulus of 205 GPa, determined from uniaxial tension test according to ASTM E8 standard [33]; Poisson's ratio of 0.29, typical for stainless steel; and density of 7830 kg/m³, obtained by the water displacement method, were used. Contact surfaces were modeled with an automatic 2D single surface configuration and assumed frictionless. Initial conditions applied to the numerical model consist of an initial velocity applied over the striker bar's nodes. Boundary conditions consist of radial displacement restriction of the nodes on all the bodies' symmetry axes. Simulation time was set to 1.0 ms, and the time step was configured

Fig. 4 Sketch of the finite element model of the SHPB test (not to scale)

STRIKER:
-Elements: PLANE162
-Material model: Linear Elastic
-Initial velocity: v_0

SPECIMEN:
-Elements: PLANE162
-Material model: Plastic Kinematic

TRANSMISSION BAR:
-Elements: PLANE162
-Material model: Linear Elastic

INCIDENT BAR:
-Elements: PLANE162
-Material model: Linear Elastic

CONTACT
-Automatic 2D single surface
-Frictionless

2D Axisymmetic model

Fig. 5 Results from quasi-static compression test

Table 5 Quasi-static mechanical properties of copper alloy UNS C83600

E (GPa)	σ_0 (MPa)	E_{tan} (MPa)	σ_{max} (MPa)	ε_f (mm/mm)
100.5	115.0	685.2	315.5	0.30

automatically. Execution time for each numerical model of the SHPB test is on average 32.8 s. Figure 4 shows a sketch of the finite element model of the SHPB test.

Results and Discussion

Quasi-static Compression Tests

Figure 5 shows results from the three quasi-static compression tests. Stress–strain curves show a linear elastic region followed by a plastic region until fracture. Mean quasi-static mechanical properties extracted from these stress–strain curves are shown in Table 5.

Split Hopkinson Pressure Bar Tests

Each performed SHPB test captured strain signals on the incident and transmission bars. Figure 6 shows the strain signals captured on both bars for the test at an average strain rate of 2714 s^{-1}. Similar strain signals were captured
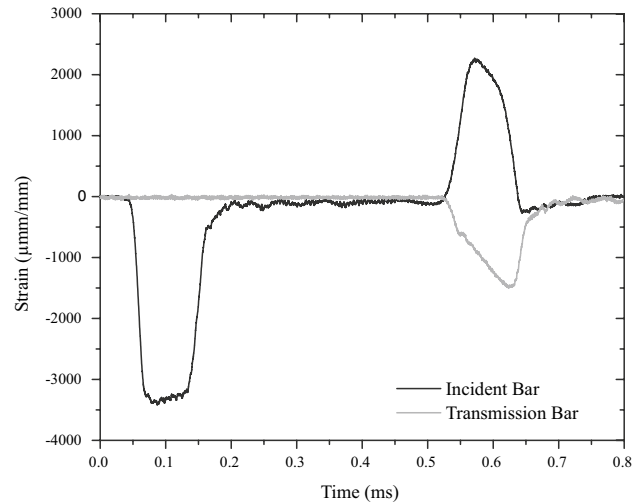
Fig. 6 Strain signals capture on bars during a SHPB test at 2714 s^{-1}

for all the experiments performed at different strain rates. Similar strain signals were captured for all the experiments performed at different average strain rates. At this point, it is worth mentioning that the theory behind the SHPB test assumes that specimens are deformed at a constant strain rate. However, in practice, strain rates are non-constant and non-uniform during deformation. This phenomenon is not well understood and continues to be an open research problem [34]. Hence, this paper uses average strain rates that conform with the original SHPB theoretical model for the proposed inverse method, which differs from the actual rates the material is experiencing. Considering the above, in estimating the parameters of the Cowper-Symonds model, we used the transmitted pulse captured from the SPHB test at 2714s^{-1}, which is close to the median of the average strain rates produced during the experiments. In the next section, it will be shown that it is possible to predict gross features of the deformation process during a Taylor Test, even with the limitation mentioned above in the current knowledge of the SHPB test. Figure 7 shows the transmitted pulse used as input in the inverse characterization process.

From the strain signals on the SHPB test, true stress-true strain curves were reconstructed. True stress-true strain curves for copper alloy UNS C83600 at different strain rates are shown in Fig. 8. This Figure shows the quasi-static curve obtained from the uniaxial compression test and four curves
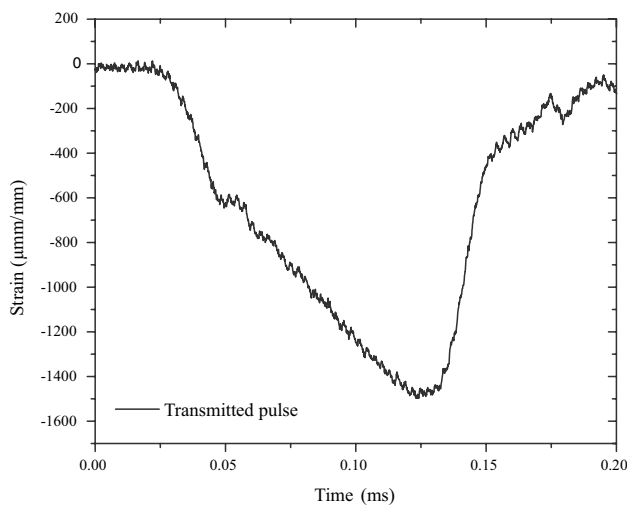
from SHPB tests at different strain rates. True stress-true strain curves at higher strain rates show a hardening behavior compared to the quasi-static curve. The yield point where the plastic region starts increases proportionally with the strain rate. However, the plastic region shows linear behavior with a tangent modulus with small increments at higher strain rates.

Taylor Test

Five Taylor specimens were impacted at different velocities. Figure 9 shows photographs of the five deformed Taylor specimens after impact. All specimens were measured, and their dimensions are shown in Table 6. The pictures show a conical shape (mushroom) at the impact end of the specimens that accentuate as the impact velocity increases. By performing a more in-depth visual inspection of the specimens, a peculiarity can be observed in this copper alloy that is not commonly observed in other metallic materials: the deformed region shows a wrinkling of the surface of the specimen.

Although the wrinkling process is not well understood, the absence of aluminum in its composition, which is necessary for the deoxidation process during raw materials manufacturing, can cause a high oxygen content that allows heterogeneous growth of dendrites and spherical discontinuities. Both defects, oxygen microspheres scattered throughout the microstructure, and the heterogeneous growth of alpha dendrites during solidification may have caused the specimen surface's wrinkling during the Taylor impact test.

Average strain rate $\dot{\varepsilon}_{avg}$ achieved during impact was calculated for each specimen according to Eq. 1, average strain rates between 2943 s^{-1} and 3804 s^{-1} were achieved.

Fig. 7 Transmitted pulse from SHPB test at 2714 s^{-1} used as input on the inverse characterization method
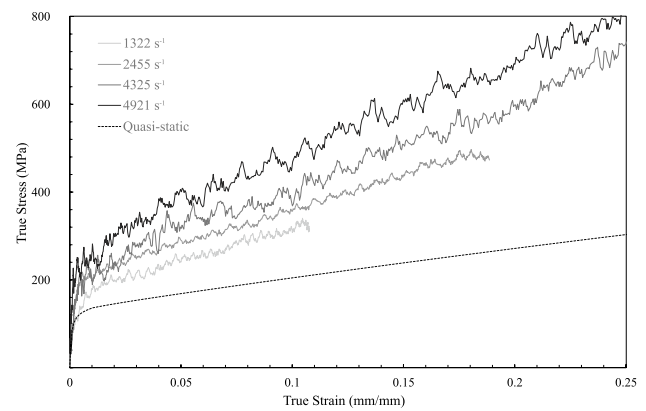
Fig. 8 Stress–strain curves at different strain rates for copper alloy UNS C83600

Additionally, the dynamic yield strength σ_y was calculated for each impact using Eq. 2 and shown in Table 6. The Taylor impact tests results show that the copper alloy UNS C83600 has a highly dependent yield strength to the strain rate. The yield strength shows a hardening behavior with the average strain rate $\dot{\varepsilon}_{avg}$. It shows high differences between the yield strength measured at the quasi-static range (115 MPa) and high strain rates (437 MPa at 3800 s^{-1}).

Constitutive Model Characterization

Parameters from Inverse Method

The proposed inverse computational identification method described in "Constitutive Model Characterization" section was employed to determine the material parameters associated with the Plastic Kinematic constitutive model for the copper alloy UNS C83600. Five material parameters were identified: the elastic modulus E, the initial yield stress σ_0, the tangent modulus E_{tan}, and the two Cowper-Symonds parameters C and P.

The inverse characterization procedure input was the transmitted pulse captured from the SHPB test at 2714 s^{-1}

Fig. 9 Taylor specimens after impact. Impact velocity: (1) 101.56 m/s, (2) 112.87 m/s, (3) 123.70 m/s (4) 131.47 m/s (5) 177.80 m/s

Table 6 Results from Taylor impact tests

Test	L_0 (mm)	D_0 (mm)	v_0 (m/s)	L_f (mm)	D_f (mm)	X (mm)	$\dot{\varepsilon}_{avg}$ (s^{-1})	σ_y (MPa)
1	25.56	8.50	101.56	22.30	10.13	8.31	2943.8	340.1
2	25.58	8.50	112.87	21.89	10.29	9.01	3405.9	367.9
3	25.71	8.50	123.70	21.70	10.30	7.76	3445.7	406.0
4	25.55	8.50	131.47	21.17	10.44	8.14	3775.7	413.5
5	25.53	8.49	144.73	20.58	11.58	6.51	3804.7	437.2

Table 7 Plastic Kinematic material parameters for copper alloy UNS C83600 determined by inverse computational method

Run	E (GPa)	σ_0 (MPa)	E_{tan} (MPa)	C (s^{-1})	P (-)	Error	Time (h)
1	95.4	194.9	1567.0	7245.9	1.00	0.0894	32.8
2	102.5	191.2	1559.8	7684.0	0.93	0.0859	22.7
3	95.3	185.2	1511.7	7151.8	1.04	0.0899	42.5
4	99.2	180.8	1550.5	7512.4	0.94	0.0887	12.9
5	96.4	176.9	1492.0	7394.5	0.90	0.0890	40.6
6	92.8	183.7	1527.9	7819.9	0.97	0.0895	23.7
7	92.2	175.8	1550.8	7313.9	0.96	0.0876	17.8
8	99.4	167.2	1510.1	7145.5	1.08	0.0899	11.3
9	96.5	188.5	1589.9	7596.5	1.05	0.0896	76.9
10	91.4	177.3	1566.8	7712.8	1.10	0.0897	65.7
Mean	96.1	182.1	1550.6	7457.7	1.00	0.0889	34.7
St. Dev.	3.5	8.3	29.4	242.7	0.07	0.003	22.14
Var. Coeff.	3.6%	4.5%	1.9%	3.3%	6.8%		

as shown in Fig. 7. The genetic algorithm was configured to use 50 individuals and 50 generations. The selection operator was the proportionate fitness selection, also known as roulette wheel selection. Three crossover operators were implemented, heuristic, arithmetic, and uniform, and used randomly. The mutation was set up to change the 40% of the individuals in each generation to prevent locking in local minimums.

Ten runs of the computational characterization procedure were executed to illustrate the optimization process's repeatability and robustness. The characterization process results for the copper alloy UNS C83600 are shown in Table 7. Parameters are shown for all ten runs, along with the error and the computational time.

The solution's error or quality is analyzed by comparing the experimental input signal with the optimization results. Figure 10 shows the comparison between the experimentally transmitted pulse and the numerical simulations using the fittest, the mean, and the worst set of material parameters (runs 2, 5, and 3, respectively). This Figure illustrates the quality of the results; the computed transmitted pulses fit the experimental pulse accurately. Indeed, the waves' differences in the main pulse and noise are observed; however, the experimental pulse's main features are captured truthfully by the computed pulses.

The robustness of the computational characterization procedure to determine the material parameters was studied
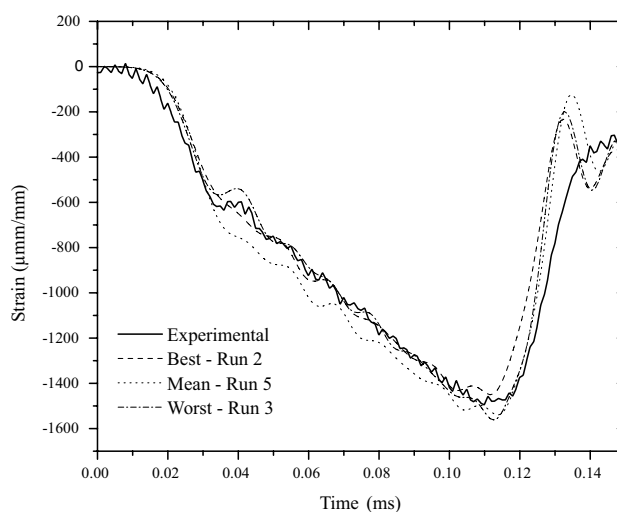
Fig. 10 Comparison between the experimental transmitted pulse at 2714 s^{-1} and the numerical simulations

by executing the characterization of the copper alloy UNS C83600 ten times. The precision uncertainty and the confidence interval with a confidence level of 95% were determined. The parameters that characterize the mechanical behavior of the copper alloy UNS C83600 at high strain rates are shown in Table 8 with a confidence level of 95%. In these terms, the characterization procedure determines the

material parameters with a mean uncertainty of 4.1% for all the parameters and a maximum uncertainty of 7.0% for the Cowper-Symonds parameter P.

According to the Plastic Kinematic constitutive model, material parameters determined by the inverse method were used to reconstruct the stress–strain curves at different strain rates. The reconstructed curves were compared with the experimental data and shown in Fig. 11. Good agreement with the experimental data was achieved.

Parameters from Curve-Fitting Method

On the other hand, the material parameters were also determined using a classic curve-fitting method to compare results. Constitutive model parameters were identified by fitting the Plastic Kinematic constitutive model to the four stress–strain curves at different strain rates obtained from the SHPB tests. Minimizing the mean squared error between the constitutive mathematical model and experimental curves was used. The elastic modulus E, the initial yield stress σ_0, the tangent modulus E_{tan}, and the two Cowper-Symonds parameters C and P were determined. Table 9 shows the constitutive material parameters for the copper alloy UNS C83600 obtained from the curve-fitting method.

Also, stress–strain curves calculated from the Plastic Kinematic constitutive model using material parameters obtained by the curve-fitting approach are shown in Fig. 11. As expected, better agreement with experimental stress–strain curves is observed.

Parameter Validation by Taylor Test Simulation

The quality of determining material parameters by both methods was validated by simulating a Taylor impact test using ANSYS/LS-DYNA. Due to the symmetry of the test, it was modeled using 2D axisymmetry. 2D structural solid elements (PLANE162), with quadrilateral shape, four nodes, and six degrees of freedom per node, were used to model the Taylor specimen. The target wall was modeled using the rigid material model with steel properties (Elastic Modulus 200 GPa, Poisson's ratio 0.27, density 7830 kg/m^3). The contact between the Taylor specimen and the rigid wall was assumed frictionless and configured with the automatic 2D single surface option.

Five Taylor test simulations at different impact velocities were computed with each parameter set (determined by the
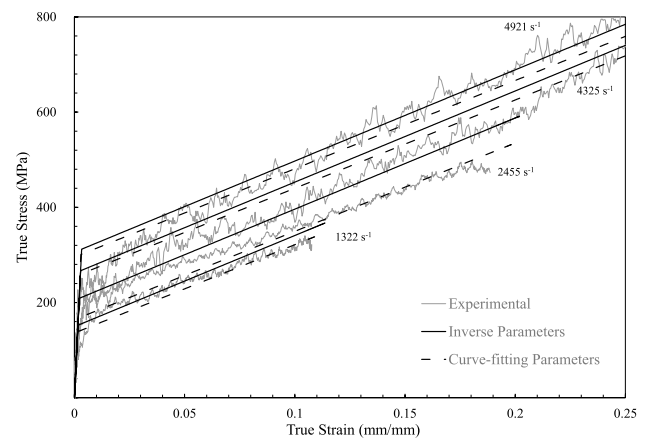
Fig. 11 Stress–strain curves for copper alloy UNS C83600 at different strain rates with the Plastic Kinematic model. Solid gray lines show the experimental curves computed from SHPB results, dotted black lines show the Plastic Kinematic model computed using parameters from curve-fitting method, and solid black lines show the Plastic Kinematic model computed using parameters from proposed inverse method

Inverse method and the Curve-fitting method) and configured with impact speed and geometry according to experiments shown in Table 4. Final specimen length (L_f), Final diameter (D_f) and Undeformed length (X) of each simulation was computed and compared against experimental results. Table 10 shows experimental and computational simulation results of Taylor tests. Relative error of simulation results against experimental results are shown in parenthesis below each value.

Results show that relative errors from simulations performed using parameters determined by the inverse method are significantly lower than errors computed from parameters determined using the curve-fitting method. While the relative mean errors between experimental results and inverse method parameters are 5.8%, 13.7% and 9.7% for the final length, final diameter and undeformed length respectively; the relative mean errors from curve-fitting parameters are 12.2%, 16.7% and 26.9%. These results show a better capability of the material parameter set determined by the proposed inverse computational method to compute simulations of events at high strain rates, such as the deformed shape of the Taylor tests specimens at different strain rates.

In this research, the effectiveness of the proposed inverse approach was measured by the fitness of the characterized

Table 8 Plastic Kinematic material parameters for copper alloy UNS C83600 determined by inverse method with a confidence of 95%

E (GPa)	σ_0 (MPa)	E_{tan} (MPa)	C (s^{-1})	P (-)
96.1 ± 3.6	182.1 ± 8.5	1550.6 ± 30.2	7457.7 ± 249.4	1.00 ± 0.07

Table 9 Plastic Kinematic material parameters for copper alloy UNS C83600 determined by curve-fitting method

E (GPa)	σ_0 (MPa)	E_{tan} (MPa)	C (s^{-1})	P (-)
102.4	127.7	1854	4276	0.468

Table 10 Results of computational simulation of Taylor Tests using parameters determined by Inverse method and by Curve-fitting method. Errors against experimental results are shown below each result in parentheses

Test	1	2	3	4	5	Mean error
v_0 (m/s)	101.56	112.87	123.7	131.47	144.73	
Experimental						
L_f (mm)	22.3	21.89	21.70	21.17	20.58	
D_f (mm)	10.13	10.29	10.30	10.44	11.58	
X (mm)	8.31	9.01	7.76	8.14	6.51	
Inverse						
L_f (mm)	23.34	23.05	22.76	22.54	22.18	
	(4.7%)	(5.3%)	(4.9%)	(6.5%)	(7.8%)	5.8%
D_f (mm)	9.02	9.04	9.06	9.08	9.20	
	(11.0%)	(12.1%)	(12.0%)	(13.0%)	(20.6%)	13.7%
X (mm)	7.47	8.17	6.74	6.68	6.64	
	(10.1%)	(9.3%)	(13.1%)	(17.9%)	(2.0%)	9.7%
Curve-fitting						
L_f (mm)	24.15	24.15	24.14	24.11	24.09	
	(8.3%)	(10.3%)	(11.2%)	(13.9%)	(17.1%)	12.2%
D_f (mm)	8.78	8.78	8.79	8.79	8.79	
	(13.3%)	(14.7%)	(14.7%)	(15.8%)	(24.1%)	16.5%
X (mm)	5.94	5.93	5.94	5.90	5.16	
	(28.5%)	(34.2%)	(23.5%)	(27.5%)	(20.7%)	26.9%

constitutive model to predict the essential deformation physics at high-strain rates during five Taylor Tests at different strain rates. For example, it was found that the mean error of the proposed approach is significantly smaller than the one found by the curve-fitting method, especially in the longitudinal direction (see Table 10). Note, the time it takes to identify the parameters was not used as an objective measure of effectiveness because it depends on the computer hardware, the CPU parallel algorithm implementation, and the finite element model setup used during the optimization process, among other factors.

The difference in the effectiveness between the curve-fitting approach and the proposed inverse one can be explained by the amount of information used to identify the parameters of the Cowper-Symonds constitutive model (Eq. 3) from SHPB experiments, as follows. The curve-fitting approach requires a set of reconstructed specimen stress–strain curves from measured transmitted and reflected strain pulses. The main disadvantage of this procedure is that to find the model's parameters, every reconstructed curve is said to be occurring at a constant strain rate (the average strain rate). This hypothesis is, in fact, a loss of information because the specimen's strain rate is non-constant and non-uniform during deformation [34].

On the other hand, the proposed inverse approach uses a single transmitted strain pulse labeled with the average strain rate for reporting purposes. However, the pulse contains information on the specimen's strain rates evolution up to a critical value of V_0/L, where V_0 is the striker impact velocity, and L is the initial length of the specimen [35]. For example, in this

research, a single strain pulse at an average strain rate of 2714 s^{-1} was used, which means that it contains information on the specimen's strain rates evolution up to 4165 s^{-1} (see Table 3).

Another point worth mentioning is the efficiency of the proposed inverse approach. Experimental work on an SHPB is a specialized technical area where the experimenter's experience is vital to reduce sources of error, like specimen positioning, bars misalignment, friction between bars and specimen, and adhesion between bars and strain gauges, among others. In practice, an experiment cannot be repeated under the same conditions, and measuring a well-formed single-strain pulse where error sources are minimized requires many trials, which can take several hours or even days. Then, using the curve-fitting approach requires more hours of experimental work to measure the set of strain pulses needed for the least-squares procedure compared to the approach that is being proposed here.

Finally, a note on the performance of the proposed inverse approach. The identified parameters were used to predict the deformation of five samples in a Taylor test at characteristic strain rates between 2943.8 s^{-1} and 3804.7 s^{-1} (see Table 6). Note that these characteristic strain rates are below the critical strain rate of the chosen SHPB experiment (4165 s^{-1}). This shows the robustness of the proposed approach.

Conclusions

Copper alloy UNS C83600 was mechanically characterized at high strain rates using experimental and computational techniques to determine its constitutive behavior. Split Hopkinson Pressure Bar tests and Taylor impact tests were performed to determine the copper alloy's mechanical behavior under strain rates of 1000 to 5000 s^{-1}. An inverse computational identification method at high strain rates using a single Split Hopkinson Pressure Bar test was used to characterize a copper alloy UNS C83600 under the Plastic Kinematic scope model. This method uses the transmitted pulse from an SHPB test as input to determine the material parameters associated with a given constitutive model.

The proposed inverse characterization method seeks to overcome three main limitations identified in the traditional curve fitting characterization procedures at high strain rates. (1) Several experimental SHPB tests are required in the characterization process, in many cases, complicated and expensive. The traditional curve fitting method requires to use at least four SHPB test at different strain rate while the proposed inverse method uses a single SHPB test to determine all material parameters. (2) Material parameters are determined sequentially, dismissing interactions among parameters. The proposed inverse method uses an optimization technique to determine all five parameters simultaneously unlike the traditional method that determines each parameter independently. (3) Input data for the characterization techniques is limited to stress–strain curves. In the case of SHPB test, to obtain stress–strain curves a model should be applied which includes another source of error. Instead, the proposed method uses as input the raw data of the transmitted pulse directly from the bars to determine the material parameters.

Results demonstrated that the inverse computational characterization method's material parameters yielded good agreement between simulations using these parameters and experimental results. Peak values of the computed transmitted pulse compared with experimental measurements showed a maximum relative error of 4.3. Likewise, the determined materials parameters by the two methods were validated by comparing the results of multiple simulations of the Taylor tests against experimentation. Results of simulated Taylor specimens computed using both sets of material parameters showed better agreement to replicate the deformed specimen shape than results computed using parameters estimated by traditional curve fitting method.

On the other hand, the uncertainty of determining parameters was maintained low. However, special attention is necessary to the two Cowper-Symonds parameters results since lower sensitivity was observed.

Declarations

References

1. Sun Y, Burgueño R, Vanderklok AJ, Tekalur SA, Wang W, Lee I (2014) Compressive behavior of aluminum/copper hybrid foams under high strain rate loading. Mater Sci Eng A 592:111–120
2. Acharya S, Gupta R, Ghosh J, Bysakh S, Ghosh K, Mondal D, Mukhopadhyay AK (2017) High strain rate dynamic compressive behaviour of Al6061-T6 alloys. Mater Charact 127:185–197
3. Wang L, Qiao J, Ma S, Jiao Z, Zhang T, Chen G, Zhao D, Zhang Y, Wang Z (2018) Mechanical response and deformation behavior of al0. 6cocrfeni high-entropy alloys upon dynamic loading. Mater Sci Eng A 727:208–213
4. Zhang W, Chen X, Zhuo B, Li P, He L (2018) Effect of strain rate and temperature on dynamic mechanical behavior and microstructure evolution of ultra-high strength aluminum alloy. Mater Sci Eng A 730:336–344
5. Kavanagh KT, Clough RW (1971) Finite element applications in the characterization of elastic solids. Int J Solids Struct 7(1):11–23
6. Mariani S, Gobat G (2019) Identification of strength and toughness of quasi-brittle materials from spall tests: a sigma-point kalman filter approach. Inverse Probl Sci Eng 27(9):1318–1346
7. Vaz M Jr, Tomiyama M (2020) Identification of inelastic parameters of the aisi 304 stainless steel: a multi-test optimization strategy. Inverse Probl Sci Eng 28(11):1551–1569
8. Field JE, Walley SM, Proud WG, Goldrein HT, Siviour CR (2004) Review of experimental techniques for high rate deformation and shock studies. Mater Sci Eng A 30(7):725–775
9. Chen WW, Song B (1989) Split Hopkinson (Kolsky) bar: design testing and applications. Springer, New York
10. Gilat A, Seidt J, Matrka T, Gardner K (2019) A new device for tensile and compressive testing at intermediate strain rates. Exp Mech 59(5):725–731
11. Sasso M, Newaz G, Amodio D (2008) Material characterization at high strain rate by hopkinson bar tests and finite element optimization. Mater Sci Eng A 487(1–2):289–300
12. Sedighi M, Khandaei M, Shokrollahi H (2010) An approach in parametric identification of high strain rate constitutive model using hopkinson pressure bar test results. Mater Sci Eng A 527(15):3521–3528
13. Milani AS, Dabboussi W, Nemes JA, Abeyaratne RC (2009) An improved multi-objective identification of Johnson-Cook material parameters. Int J Impact Eng 36(2):294–302
14. ASTM: ASTM standard E478-08(2008)-Standard test methods for chemical analysis of copper alloys
15. ASTM: ASTM designation B62-09(2009)-Standard specification for composition bronze or ounce metal castings
16. ASTM: ASTM standard E9-09 (2009)-standard test methods of compression testing of metallic materials at room temperature
17. Kolsky H (1949) An investigation of the mechanical properties of materials at very high rates of loading. Proc Phys Soc Sect B 62(11):676–700
18. Hopkinson B (1914) A method of measuring the pressure produced in the detonation of high explosives or by the impact of bullets. Proc R Soc Lond Ser A 89(612):411–413
19. Davies RM (1948) A critical study of the Hopkinson pressure bar. Philos Trans R Soc Lond Ser A 240(821):375–457

20. Taylor GI (1948) The use of flat-ended projectiles for determining dynamic yield stress. I. Theoretical considerations. Proc R Soc Lond Ser A 194(1038):289–299

21. Meyers MA (1994) Dynamic Behavior of Materials. Wiley-Interscience, New York

22. Whiffin AC (1948) The use of flat-ended projectiles for determining dynamic yield stress. II. Tests on various metallic materials. Proc R Soc Lond A 194:300–322

23. Wilkins ML, Guinan MW (1973) Impact of cylinders on a rigid boundary. J Appl Phys 44(3):1200–1206

24. Hawkyard JB (1969) A theory for the mushrooming of flat-ended projectiles impinging on a flat rigid anvil, using energy considerations. Int J Mech Sci 11(3):313–333

25. ANSYS: ANSYS LS-DYNA User's Guide: ANSYS Release 12.0. ANSYS Inc., (2009). ANSYS Inc

26. Cowper GR, Symonds PS (1957) Strain hardening and strain-rate effects in the impact loading of cantilever beams. Technical Report 28, Brown University Division of Applied Mathematics

27. Hernandez C, Maranon A, Ashcroft I, Casas-Rodriguez J (2013) A computational determination of the Cowper-Symonds parameters from a single Taylor test. Appl Math Modell 37(7):4698–4708

28. Hernandez C, Buchely M, Maranon A (2015) Dynamic characterization of Roma Plastilina No. 1 from Drop Test and inverse analysis. Int J Mech Sci 100:158–168

29. Acosta C, Hernandez C, Maranon A, Casas-Rodriguez J (2016) Validation of material constitutive parameters for the AISI 1010 steel from Taylor impact tests. Mater Des 110:324–331

30. Lambert G, Gao H (1995) Line moments and invariants for real time processing of vectorized contour data. In: Braccini C, DeFloriani L, Vernazza G (eds) Image analysis and processing. Lecture notes in computer science. Springer, New York, pp 347–352

31. Hu MK (1962) Visual pattern recognition by moment invariants. IRE Trans Inform Theory 8(2):179–187

32. Wen W, Lozzi A (1993) Recognition and inspection of manufactured parts using line moments of their boundaries. Pattern Recognit 26(10):1461–1471

33. ASTM: ASTM Standard E8/E8M-22-Standard test methods for tension testing of metallic materials (2022)

34. Shin H, Kim J-B (2019) Evolution of specimen strain rate in split Hopkinson bar test. Proc Inst Mech Eng Part C 233(13):4667–4687

35. Gray G III, Blumenthal WR (2000) Split-hopkinson pressure bar testing of soft materials. ASM Handbook 8:488–496